

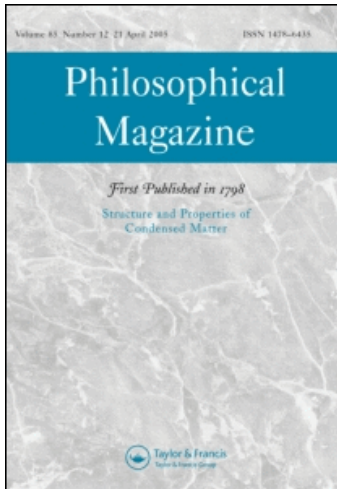
This article was downloaded by: [CAS Chinese Academy of Sciences]

On: 29 November 2008

Access details: Access Details: [subscription number 790943593]

Publisher Taylor & Francis

Informa Ltd Registered in England and Wales Registered Number: 1072954 Registered office: Mortimer House, 37-41 Mortimer Street, London W1T 3JH, UK



Philosophical Magazine

Publication details, including instructions for authors and subscription information:

<http://www.informaworld.com/smpp/title-content=t713695589>

Combined effects of crystallographic orientation, stacking fault energy and grain size on deformation twinning in fcc crystals

W. Z. Han ^a; Z. F. Zhang ^a; S. D. Wu ^a; S. X. Li ^a

^a Shenyang National Laboratory for Materials Science, Institute of Metal Research, Chinese Academy of Sciences, China

First Published: August 2008

To cite this Article Han, W. Z., Zhang, Z. F., Wu, S. D. and Li, S. X. (2008) 'Combined effects of crystallographic orientation, stacking fault energy and grain size on deformation twinning in fcc crystals', *Philosophical Magazine*, 88:24, 3011 — 3029

To link to this Article: DOI: 10.1080/14786430802438168

URL: <http://dx.doi.org/10.1080/14786430802438168>

PLEASE SCROLL DOWN FOR ARTICLE

Full terms and conditions of use: <http://www.informaworld.com/terms-and-conditions-of-access.pdf>

This article may be used for research, teaching and private study purposes. Any substantial or systematic reproduction, re-distribution, re-selling, loan or sub-licensing, systematic supply or distribution in any form to anyone is expressly forbidden.

The publisher does not give any warranty express or implied or make any representation that the contents will be complete or accurate or up to date. The accuracy of any instructions, formulae and drug doses should be independently verified with primary sources. The publisher shall not be liable for any loss, actions, claims, proceedings, demand or costs or damages whatsoever or howsoever caused arising directly or indirectly in connection with or arising out of the use of this material.

Combined effects of crystallographic orientation, stacking fault energy and grain size on deformation twinning in fcc crystals

W.Z. Han*, Z.F. Zhang, S.D. Wu* and S.X. Li

*Shenyang National Laboratory for Materials Science, Institute of Metal Research,
Chinese Academy of Sciences, Shenyang, China*

(Received 25 January 2008; final version received 26 August 2008)

The combined effects of crystallographic orientation, stacking fault energy (SFE) and grain size on deformation twinning behavior in several face-centred cubic (fcc) crystals were investigated experimentally and analytically. Three types of fcc crystals, Al single crystals, Cu single crystals and polycrystalline Cu–3% Si alloy with different SFEs and special crystallographic orientations, were selected. The orientations of the Al and Cu single crystals were designed with one of the twinning systems (111)[$\bar{1}\bar{1}2$] just perpendicular to the intersection plane of equal-channel angular pressing (ECAP). For Al single crystals, no deformation twins were observed after a one-pass ECAP, although a preferential crystallographic orientation was selected for twinning. For Cu single crystals, numerous deformation twins were found even when strained at room temperature and at low strain rate. For Cu–3% Si alloy, deformation twins were only observed in some grains; however, others with different orientations were full of dislocations, although it has the lowest SFE value of the three fcc crystal types. The experimental results provide evidence that SFE and crystallographic orientation have a remarkable influence on the behavior of deformation twinning in fcc crystals. The observations were subsequently analyzed based on fundamental dislocation mechanisms and the grain-size effect. The deformation conditions required for twinning and the variation in twinning stress with SFE, crystallographic orientation and grain size in fcc crystals are also discussed.

Keywords: equal channel angular pressing (ECAP); deformation twin; FCC crystal; stacking fault energy; grain size

1. Introduction

Twinning is a frequent and important mechanism for plastic deformation in crystalline materials [1–5]. Deformation twins have long been known in body-centred cubic (bcc), hexagonal close-packed (hcp) and other crystals with lower symmetry, but are now frequently found to form in many fcc metals and alloys [3–5]. Since Blewitt et al. [6] reported that deformation twinning occurred in Cu single crystals under tension at very low temperatures, numerous investigations have been conducted to better understand the twinning mechanism in various face-centred cubic (fcc) metals [7–27]. It is well known that the twinning behavior of fcc crystals is strongly affected by the stacking fault energy (SFE)

*Corresponding authors. Email: wzhan@imr.ac.cn or shdwu@imr.ac.cn

[7–11]. Deformation twinning is easier in fcc crystals with very low SFE value, but becomes more difficult in the fcc crystals with medium to high SFE value [7–11]. In addition, deformation twinning does not take place under conventional deformation conditions, such as tension, compression or torsion at room temperature (RT) and/or at low strain rate, etc. in fcc metals with medium to high SFE values. For example, normally there are no deformation twins in coarse-grained Cu, Cu–2% Al, Al or its alloys strained under conventional loading conditions [2,7,10]. However, deformation twins are readily found when metals or alloys are loaded at low temperature [6,12] and/or at a high strain rate [13–18]. It was recently found that deformation twinning occurs easily in ultrafine- or nano-grained materials [19–27]. Molecular dynamic (MD) simulations predicted that, in nanocrystalline (NC) Al and Cu, twins should nucleate preferentially via the process of successively emitting partial dislocations [19–22]. These predictions were subsequently verified in NC Al film and in NC Cu [22–27], indicating that grain size also influences twinning behavior. The existing experimental results indicate that many extrinsic and intrinsic factors, such as SFE, grain size, deformation mode, strain, strain rate, temperature, etc. have a significant influence on deformation-twinning preferences.

Concerning intrinsic factors, the above discussion shows that SFE and grain size are two key factors for deformation twinning in fcc crystals. However, several contradictory conclusions have been drawn in previous investigations. Firstly, since SFE has a significant influence on deformation twinning behavior [7–11], and the lower the SFE is, the easier deformation twinning occurs, numerous deformation twins should be readily observed in low-SFE materials. However, it is unclear why deformation twins are observed only in some grains in low-SFE Cu–Al alloy during tension, while other grains of similar size lack deformation twins [8]. Secondly, Meyers et al. [13] found that numerous twins were obtained at grain sizes of 117 and 315 μm in Cu during shock compression experiments, but virtually no twins appeared at a grain size of 9 μm . Similarly, in MP35N alloy, no twins were found when the grain size was smaller than 1 μm [11]. These findings imply that deformation twinning in fcc materials becomes very difficult as the grain size decreases to a certain scale. On the other hand, both MD simulations [19–22] and experimental results have demonstrated that deformation twins readily nucleate in pure Al and Cu crystals, even though their grains are submicrometer in size [22–27]. Obviously, these results are confusing, and therefore, it is unclear whether a small grain size is a promoting factor for nucleating deformation twins during plastic deformation. Thirdly, it is generally assumed that the process of deformation twinning often competes with dislocation slip. Thus, several models were proposed to predict the preference for twinning in NC materials [23–27]. It was suggested that twinning would become a preferential deformation mode in NC materials when the grain size is smaller than a critical value. However, experimental results have indicated that deformation twinning only occurred in some grains, while, according to the model prediction, twins should widely exist in NC materials when the grain size is below a critical value [23–27]. It is also well known that crystallographic orientation, as an important intrinsic factor, has a significant influence on dislocation slip behavior during plastic deformation [28–30]. The effect of crystallographic orientation on the behavior of deformation twinning is less investigated [6]. Deformation twins were not observed in Cu single crystals, when subjected to tension along the $\langle 123 \rangle$ orientation at low temperature, until the axis rotated into an orientation where co-planar secondary slip occurred [6]. However, no deformation twins were observed in copper single crystals when subjected to tension at RT. Therefore, further study is necessary to assess how SFE, grain

size and crystallographic orientation affect deformation twinning during plastic deformation in fcc crystals.

In the present study, we conducted a series of experiments to show the combined effects of crystallographic orientation, grain size and SFE on deformation twinning behavior under identical external deformation conditions. Further analyses were carried out to illustrate the combined effects of SFE, grain size and crystallographic orientation on deformation twinning in three types of fcc crystal.

2. Experimental procedure

To study the combined effects of SFE and crystallographic orientation on deformation twinning behavior, three types of fcc crystal with different SFE were selected as follows: Al (166 mJ/m^{-2}), Cu (45 mJ/m^{-2}) and Cu-3% Si alloy (3 mJ/m^{-2}) [31]. The orientations of the Al and Cu single crystals were especially selected. According to the shear plane and shear direction of ECAP [32–35], we purposely located one of the twinning systems $(111)[\bar{1}\bar{1}2]$ just on the normal plane of intersection of ECAP, as illustrated in Figure 1. In this case, the twinning system would acquire the largest resolved shear stress during extrusion. The Cu-3% Si alloy used in this study is a polycrystalline sample with large initial grain size (several millimeters). Samples of Al and Cu single crystals of $8 \times 8 \times 40 \text{ mm}$ were cut according to the design in Figure 1. The Cu-3% Si alloy billet of the same dimensions consisted of two or three grains in cross-section. These crystals were then extruded by a single-pass right-angle ECAP die at RT with an extrusion rate of 5 mm/min and lubrication of MoS_2 . After ECAP, microstructural characterizations were performed using transmission electron microscope (TEM; JEM-2000FXII) and scanning electron microscope (SEM; Cambridge S-360). Thin foils for TEM and the samples for SEM were focused on the ID–ED plane (the $(\bar{1}10)$ crystallographic plane only; ID, insert direction; ED, extrusion direction; see Figure 1) in the centre of the pressed rods according to the design in Figure 1, in which the ID and ED directions are defined. Firstly, the prepared

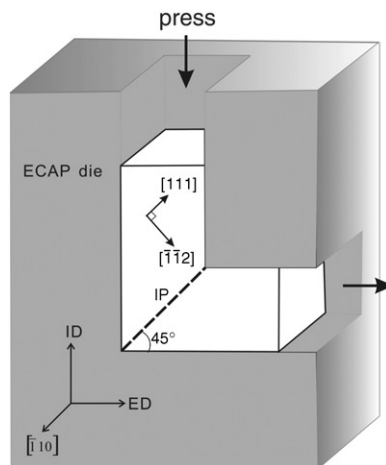


Figure 1. Schematic illustration of the ECAP coordinates and current experimental design (ID for insert direction and ED for extrusion direction).

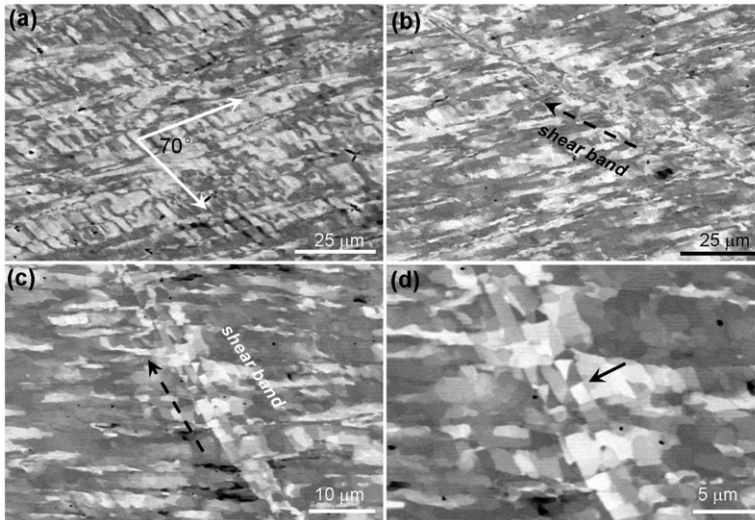


Figure 2. Typical SEM electron channelling contrast micrographs of deformation microstructures of an Al single crystal after single-pass ECAP. (a) Coarse ribbon structures and (b)–(d) shear bands formed during extrusion.

thin foils were mechanically ground to $\sim 50\ \mu\text{m}$ thick and finally thinned by a twin-jet polishing method. The samples for SEM experiments were mechanically ground using abrasive paper and, finally, electro-polished.

3. Experimental results

3.1. Al single crystal

Figure 2 shows the microstructural morphology of an Al single crystal after single-pass ECAP. Banded structures in two directions were formed on the ID–ED plane of the pressed rod, as shown in Figure 2a. The banded structures were $\sim 4\ \mu\text{m}$ wide with an intersecting angle of $\sim 70^\circ$ between the primary and secondary bands. In other regions of the observed area, narrow shear bands were scarce, as shown in Figure 2b. Observations at higher magnifications revealed that regular-shaped grains are formed within these shear bands, as displayed in Figures 2c and d. These grains, with obvious recrystallization features, differ from the general structures after severe plastic deformation [2], indicating that recrystallization takes place during the extrusion process.

Figure 3 shows a typical TEM image of a narrow shear band in the pressed Al single crystal. The microstructures in the shear band have different elongation directions compared with those around them. Part of the shear band consists of equiaxed subgrain structures rather than the ordinary elongated ribbon structure, as indicated by the arrows in Figure 3. The corresponding selected area diffraction (SAD) pattern near the shear band region indicates that the misorientations among those microstructures are small. Figure 4 is a magnified image of the region at the side of shear band. Clear dislocation configurations can be seen at the grain boundaries and in the subgrain interior. Figures 4b–d shows a magnified morphology of the area marked by the circle

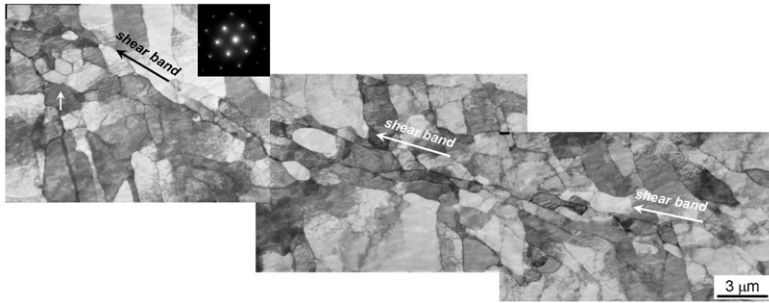


Figure 3. TEM micrographs of a narrow shear band formed in an Al single crystal during extrusion.

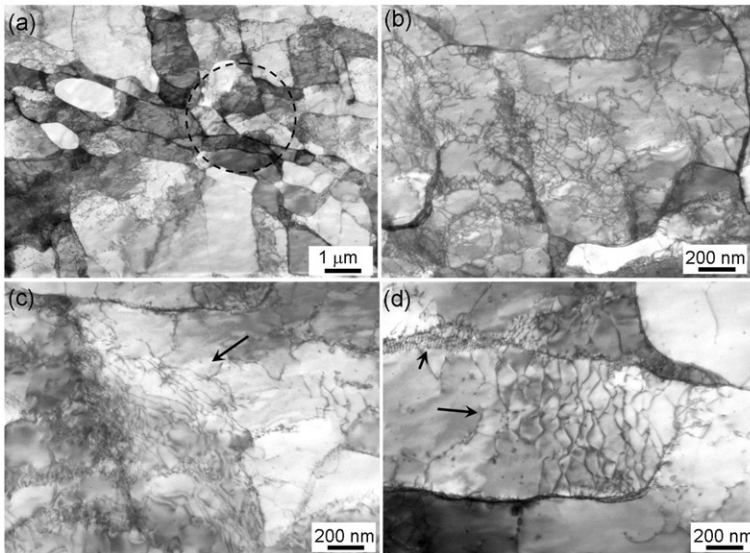


Figure 4. TEM micrographs of the dislocation configurations at the side of a shear band. (a) Low magnification morphology and (b)–(d) high magnification dislocation patterns.

in Figure 4a. Many dislocations were pinned by the grain boundary, as shown in Figures 4c and d. Dislocation tangles and a group of wavy dislocation configurations can be clearly seen in the subgrain interior. However, deformation twins were not observed in the deformed Al single crystals, although a twinning system was purposely located on one of the macroscopic shear deformation planes during extrusion [32–35]. Our results are consistent with previous investigations on Al and Al alloys strained by severe plastic deformation methods, confirming that deformation twins do not nucleate due to the high SFE value [2,7,17,34,36,37].

3.2. Cu single crystal

Figure 5 shows the microstructural morphology of a Cu single crystal after single-pass ECAP. Dense shear bands were formed on the ID–ED plane of the Cu single crystal

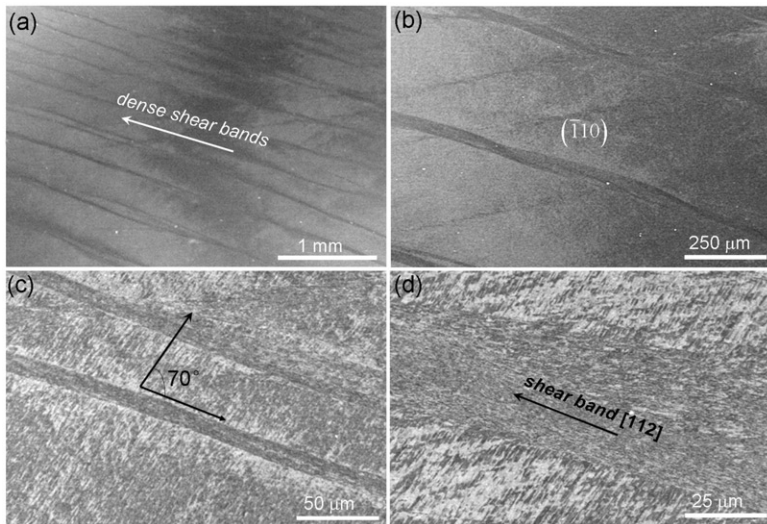


Figure 5. Typical SEM electron channelling contrast micrographs of dense shear bands formed on the ID–ED plane of a Cu single crystal during the ECAP process. (a) Macroscopic SEM image and (b)–(d) magnified SEM images.

during the process of extrusion, as shown in Figure 5a. These shear bands range in width from 10 to 50 μm , with an intersecting angle of $\sim 20^\circ$ with respect to the extrusion direction. Observations at high magnification reveal that numerous band structures were formed. The shear bands consist of very fine strip structures stretching along the propagating direction of shear deformation. The matrix region is composed of a group of slightly coarse ribbons, as shown in Figures 5b–d. The coarse ribbons make an angle of $\sim 70^\circ$ with respect to the direction of the shear bands, as shown in Figures 5c and d.

Further observations on the matrix and shear bands via TEM are shown in Figure 6. Figure 6a displays a typical image at the interface between the matrix and shear band, in which the black dashed line marks the interface. Fine banding structures in different directions are recognized in the area of matrix and shear band, which is consistent with the results shown in Figure 5. The ribbon structures in the area of matrix are divided by dense dislocation walls of ~ 500 nm in width, as indicated in Figure 6b. The corresponding SAD pattern indicates that these dislocation walls are formed along a (111) plane. The misorientation angles between the subgrain structures are very small, as evidenced by the sharp diffraction spots. This region has a high density of dislocations, which is a common feature of the metals subjected to severe plastic deformation [2,24]. However, the microstructures in the area of the shear bands are very fine, consisting of a series of strip structures with a width of < 500 nm and aligned along the direction of the shear bands (Figure 6c). The SAD pattern consists of diffraction rings (Figure 6c), indicating that the misorientation angles between the strips are large. From the initial crystallographic orientation, it is easy to decipher that the shear bands propagate along the $[\bar{1}\bar{1}2]$ crystallographic direction only [38].

Numerous deformation twins were found in the Cu single crystal after a single-pass ECAP only, as shown in Figure 7a–c. Detailed observations indicate that the deformation

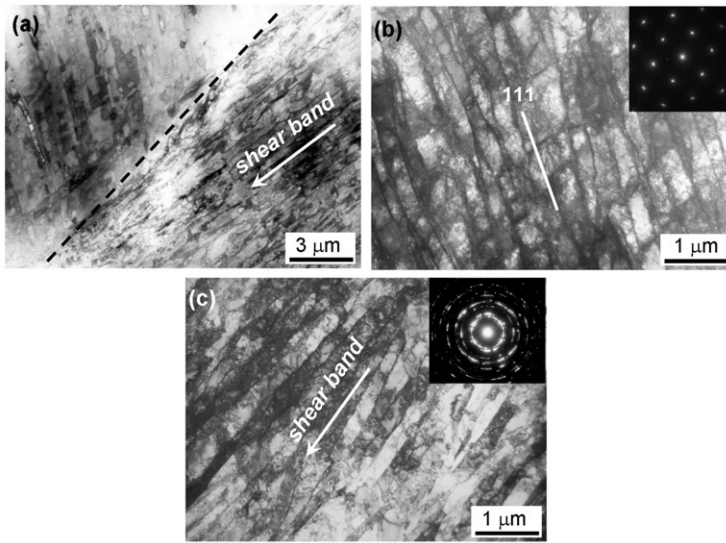


Figure 6. TEM micrographs of the deformation microstructures for a Cu crystal. (a) Image of the interface between matrix and shear band, (b) dense dislocation walls formed in the matrix region and (c) fine strip structures in the shear band.

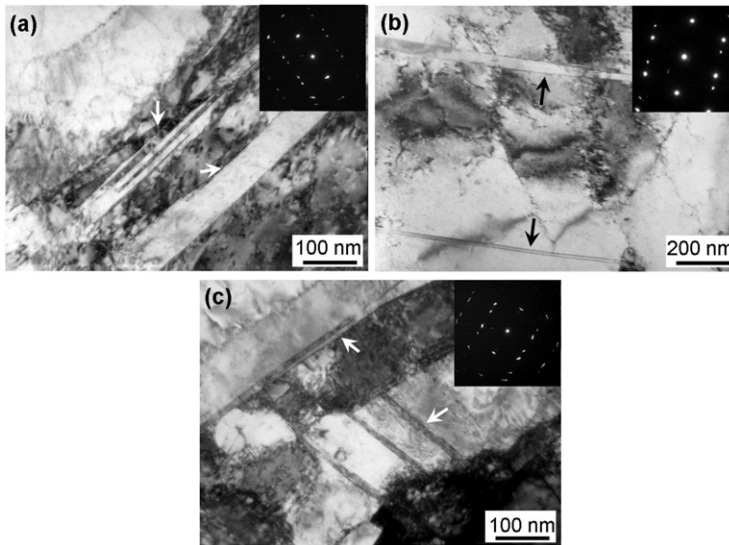


Figure 7. TEM micrographs of (a) Type I, (b) Type II and (c) Type III deformation twins formed in a Cu single crystal.

twins can be categorized into three groups according to their location and morphology, as described in detail elsewhere [38]. As expected, numerous deformation twins were generated in the Cu single crystal. Huang et al. [24] previously observed deformation twins in some grains of ECAP-ed coarse-grained Cu, while our experimental results demonstrate

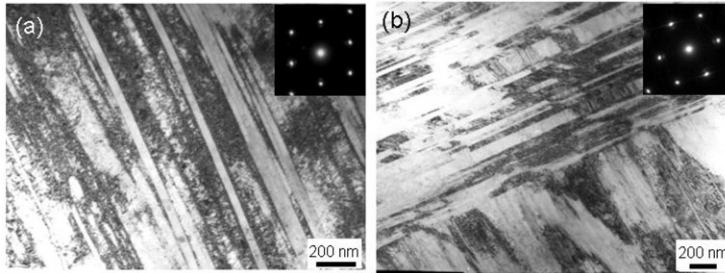


Figure 8. TEM micrographs of the planar slip features in the Cu–3% Si alloy after single-pass ECAP. (a) one direction of planar slip; (b) two directions of planar slip.

that a Cu single crystal can also deform by twinning at a low strain rate and RT when a proper crystallographic orientation is selected with respect to the ECAP die. On the other hand, in a series of Cu single crystals with random orientations processed at RT and low strain rate by ECAP [24,29] or other deformation methods [40,41], few deformation twins or no twins were found, indicating that crystallographic orientation plays a critical role in the formation of deformation twins.

3.3. Cu–3% Si alloy

Figures 8–10 show the microstructural morphologies of the Cu–3% Si alloy billet after a single-pass ECAP. Because the initial microstructures of Cu–3% Si alloy consist of several large grains, different microstructural features were observed in different grains. Figure 8 shows the microstructures of a random grain, where clear dislocation slip features can be seen within this region. A large number of dislocations are pinned by the banding structures, which are formed as the result of slip, as shown in Figure 8a. The corresponding SAD pattern demonstrates that the misorientations between these banding structures are small. Figure 8b shows an example where a secondary dislocation slip occurred within a wide band. The secondary dislocation slip traces make an angle of $\sim 70^\circ$ with respect to the primary slip traces. No deformation twins were found in this region, although the Cu–3% Si alloy has very low SFE [31].

Figure 9 shows the microstructures of another random grain. Only dislocation slip features were observed at a low magnification, as shown in Figure 9a. Observations at higher magnification demonstrate that a large number of fine deformation twins and stacking faults (SFs) exist within the narrow banding structures (Figure 9b), similarly to previous investigations [42,43]. Figures 9c and d show a group of SF images observed from the [001] direction. Narrow to wide SFs were found in this region, which had angles of $\sim 70^\circ$ with respect to each other, resulting from the activation of different twinning systems.

Figure 10 shows the microstructures in a random grain deformed mainly by twinning during extrusion. A high density of deformation twins were found within a wider banding structure, as shown in Figure 10a. Figures 10b and c are higher magnification images of the morphology at the boundary region and central part, respectively. Figure 10d is the corresponding dark-field image. SAD patterns confirm the presence of numerous

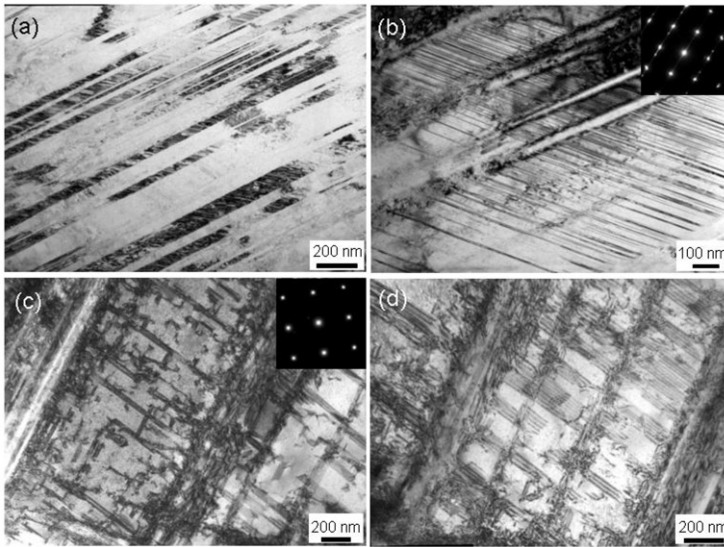


Figure 9. TEM micrographs of the numerous twins and SFs formed within the narrow banding structures in the Cu-3% Si alloy. (a,b) Fine twins and SFs in the banding structures and (c,d) images of SFs viewed from the [001] direction.

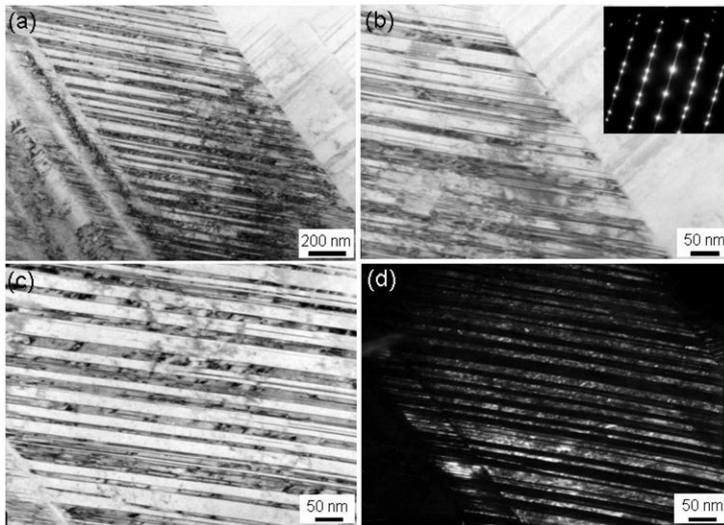


Figure 10. TEM micrographs of the deformation twins formed in the deformed Cu-3% Si alloy. (a) Low magnification image, (b) high magnification image at boundary of the band, (c) high magnification image in the inner part and (d) the corresponding dark-field image.

deformation twins and SFs. Due to differences in orientation, some grains only deform by dislocation slip, although the Cu-3% Si alloy has a very low SFE; others deform initially by dislocation slip, then the twins and SFs nucleate in those relatively fine banding structures.

4. Discussion

4.1. Dislocation reactions for nucleating Shockley partials

Our experimental results and related studies [7–27] demonstrate that SFE, crystallographic orientation and grain size significantly influence the behavior of deformation twinning in fcc crystals. However, the mechanism by which these factors affect the process of deformation twinning or the relationship between them is still unclear. To answer these questions, it is necessary to consider the dislocation reaction mechanisms.

Deformation twinning is the result of Shockley partial dislocation movement [4,5,44,48]. Two types of dislocation reactions can produce Shockley partial dislocations in fcc metals [44]. One is

$$\frac{1}{2}[\bar{1}10] \rightarrow \frac{1}{6}[\bar{2}11] + \frac{1}{6}[\bar{1}2\bar{1}], \quad (1)$$

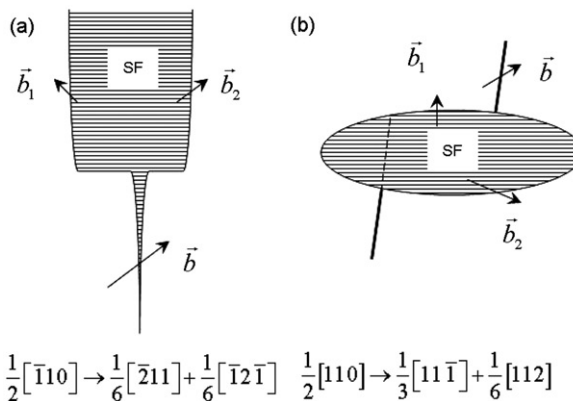
by which a perfect dislocation dissociates into two Shockley partial dislocations, leaving a stacking fault between the two partials, as schematically illustrated in Figure 11a. Such a structure is known as an extended dislocation. Another dislocation reaction is

$$\frac{1}{2}[110] \rightarrow \frac{1}{3}[11\bar{1}] + \frac{1}{6}[112], \quad (2)$$

where a perfect dislocation dissociates into a Frank and a Shockley partial dislocation, respectively, as illustrated in Figure 11b. Frank partial dislocation can not move during deformation because its Burger vector is perpendicular to the slip plane only, forming a pole. On the other hand, the Shockley partial will move around the pole under the driven stress, leaving behind a SF. This twinning model is known as the pole mechanism [4,47,48].

4.2. The role of stacking fault energy

The most common dislocation responsible for slip deformation in fcc metals is the $\frac{1}{2}\langle 110 \rangle$ dislocation [44]. However, the core of this dislocation usually splits into two Shockley



$$\frac{1}{2}[\bar{1}10] \rightarrow \frac{1}{6}[\bar{2}11] + \frac{1}{6}[\bar{1}2\bar{1}] \quad \frac{1}{2}[110] \rightarrow \frac{1}{3}[11\bar{1}] + \frac{1}{6}[112]$$

Figure 11. Schematic illustration of the dislocation reaction for nucleating partials. (a) Perfect dislocation dissociated into two Shockley partials and (b) perfect dislocation dissociated into a Frank and a Shockley partial.

partial dislocations, with a Burgers vector of $\frac{1}{6}\langle 112 \rangle$ and connected by a stacking fault. For this dissociation, an equilibrium separation between the two partials can be determined by a balance between the repulsive forces of the two Shockley partials and the attractive force of the SFE [44–49]. Therefore, the equilibrium split distance can be approximately expressed as

$$d = \frac{Gb_p^2}{8\pi\gamma}, \tag{3}$$

where $b_p = a_0/\sqrt{6}$ is the magnitude of the Burgers vector of the Shockley partials, a_0 is the lattice parameter, G is the shear modulus, and γ is the SFE. When an appropriate external shear stress is applied, the split distance between the Shockley partials may increase or decrease, depending on the type of stress. Here, we only consider the increasing case [44–46], given by the follow equation:

$$d = \frac{G}{8\pi} \frac{b_p^2}{\gamma - \tau b_p}, \tag{4}$$

where τ is the applied shear stress. Therefore, the split distance is a function of the applied stress and the value of SFE. SFE is the intrinsic factor of the materials, while the applied stress represents the corresponding external deformation conditions.

It can be seen that the split distance increases with increasing applied shear stress. If the applied stress increases to a critical value, the split distance will approach infinity. We now assess this scenario for Al, Cu and the Cu–3% Si alloy. Figure 12 shows the dependence of split distance on applied shear stress for Al, Cu and the Cu–3% Si alloy, calculated

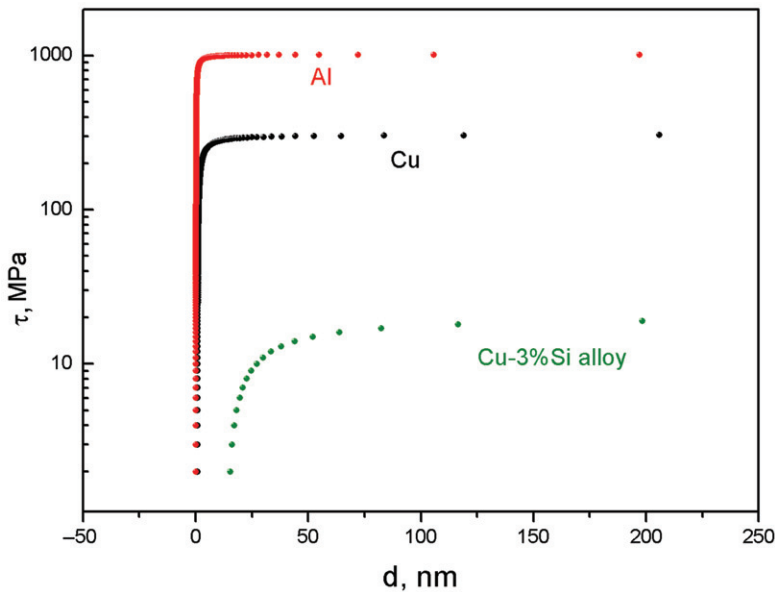


Figure 12. Plot for the split distance of an extended dislocation with increasing applied shear stress for: Al [$G = 35$ GPa], Cu [$G = 48.3$ GPa] and Cu–3% Si alloy [$G = 48.3$ GPa].

by Equation (4). A critical value of shear stress clearly exists, above which the propagation of SF is catastrophic. The plot demonstrates the presence of a critical value for nucleating a wide SF in metals with different SFEs. In general, forming a wide SF is the prerequisite step of nucleation of a deformation twin. Therefore, the required twinning stress must be greater than this critical value, which will be estimated below. In the case of $d \rightarrow \infty$ in Equation (4), one gets

$$\gamma - \tau b_p \rightarrow 0, \quad (5)$$

then yields

$$\tau_{\text{critical}} = \frac{\gamma}{b_p}. \quad (6)$$

The above analysis is for the case of the first dislocation reaction in Equation (1). For the second dislocation reaction (Equation (2)), the dissociation process can only occur if stress-driven. Therefore, the applied stress should be balanced with the increased surface energy, such that

$$\tau b_p = \gamma. \quad (7)$$

Then, the critical stress for activating the Shockley partials in the second reaction is the same as the first. Therefore, twinning stress can be written as

$$\tau_T \geq \tau_{\text{critical}} = \frac{\gamma}{b_p}. \quad (8)$$

According to Equation (8), the twinning stress for Al should be greater than 1000 MPa and higher than 300 MPa for Cu, but only larger than 20 MPa for the Cu–3% Si alloy. Twinning stresses in different metals vary significantly and SFE values have a significant influence on twinning stress. To ascertain whether deformation twinning can nucleate, two aspects need to be considered: the value of twinning stress in a metal and whether the corresponding deformation conditions can provide the required internal stress. For Al and Cu, it is easy to understand why deformation twins are produced in Cu but not in Al. The internal stress is ~ 400 MPa according to an evaluation based on dislocation density in deformed Cu [24]. This value is higher than the required Cu twinning stress (~ 300 MPa), as mentioned above. Therefore, deformation twinning can easily nucleate in severely strained coarse-grained Cu. However, for Al, due to the high SFE value, cross slip is very common during extrusion; hence, screw dislocation annihilation can occur easily. In addition, recovery and recrystallization can also take place easily during RT deformation because the Al crystal has a low melting point. Therefore, it is difficult to accumulate a high density of dislocations during extrusion; as a result, the internal stress is always maintained at a relatively low level. On the other hand, twinning stress is very high in Al according to the above estimation (> 1000 MPa). In other words, a contradiction between supply (external stress) and demand (required twinning stress) exists. Hence, in this experiment, nucleation of deformation twins is difficult in an Al single crystal.

4.3. Role of crystallographic orientation

The above analysis illustrates why deformation twins nucleate in Cu single crystals, but not in Al single crystals, during ECAP deformation in the current experiment. However, it is still unclear why numerous deformation twins are formed in the studied Cu single crystal, while other researchers found very few or no deformation twins in their experiments [39–41]. Also, deformation twins were only found in some grains of the NC materials, but according to other analyses [23–27], deformation twins will nucleate easily when the grain size reaches a critical value. To understand these issues, the effect of crystallographic orientation should be taken into consideration. Since the resolved shear stress is mainly affected by orientation [1,50], the split distance (Equation (4)) can be rewritten as

$$d = \frac{G}{8\pi\gamma - m\tau b_p} \frac{b_p^2}{}, \quad (9)$$

where m is the shear factor. Its value depends on the relationship between shear plane/shear direction and twinning plane/twinning direction, such that $m = \cos\theta\cos\beta$, where θ is the angle between the shear direction and the twinning direction and β is the angle between the two normals to the shear and twinning planes [34,38,51]. Let us consider the four cases of $m = 1, 0.75, 0.5,$ and 0.38 in the following analysis. According to Equation (9), Figure 13a depicts the variation in twinning stress of Al with crystallographic orientation (or shear factor m). It can be seen that the twinning stress value changes significantly with orientation (or shear factor m), from 1000 MPa ($m = 1$) to 2600 MPa ($m = 0.38$), indicating that deformation twinning in Al must be very difficult. Only grains with preferential orientations can deform by twinning under extremely confined deformation conditions, such as in NC Al under high-pressure indentation [23]. Figure 13b shows the changes in twinning stress with crystallographic orientation in Cu. The twinning stress is below 400 MPa for those grains with a shear factor greater than 0.75; for other grains with a lower shear factor, the twinning stress is increased significantly. For Cu single crystals, we purposely located the twinning systems in accordance with the macro-shear deformation of ECAP; i.e. the value of shear factor m is ~ 1 . As a result, the required twinning stress should be less than 400 MPa, which can be supplied during the ECAP deformation [24]. Therefore, numerous deformation twins were observed in our Cu single crystal. Figure 13c shows the relationship between twinning stress and crystallographic orientation in the Cu–3% Si alloy. Although the Cu–3% Si alloy has the lowest value of SFE, the twinning stress still needs 60 MPa (considering the effect of SFE and orientation only, not including the size effect) in some grains with a lower shear factor. This may be why some grains still deformed mainly via dislocation slip rather than twinning, as shown in Figure 8. The analysis above demonstrates that crystallographic orientation has a significant influence on the behavior of deformation twinning.

4.4. Role of grain size

The effect of grain size has been considered to illustrate the occurrence of deformation twins in nano-grained Cu, Al, Ni, etc., [23–27]. The preference for twinning or SF formation in NC grains can be understood by comparing the critical shear stress required

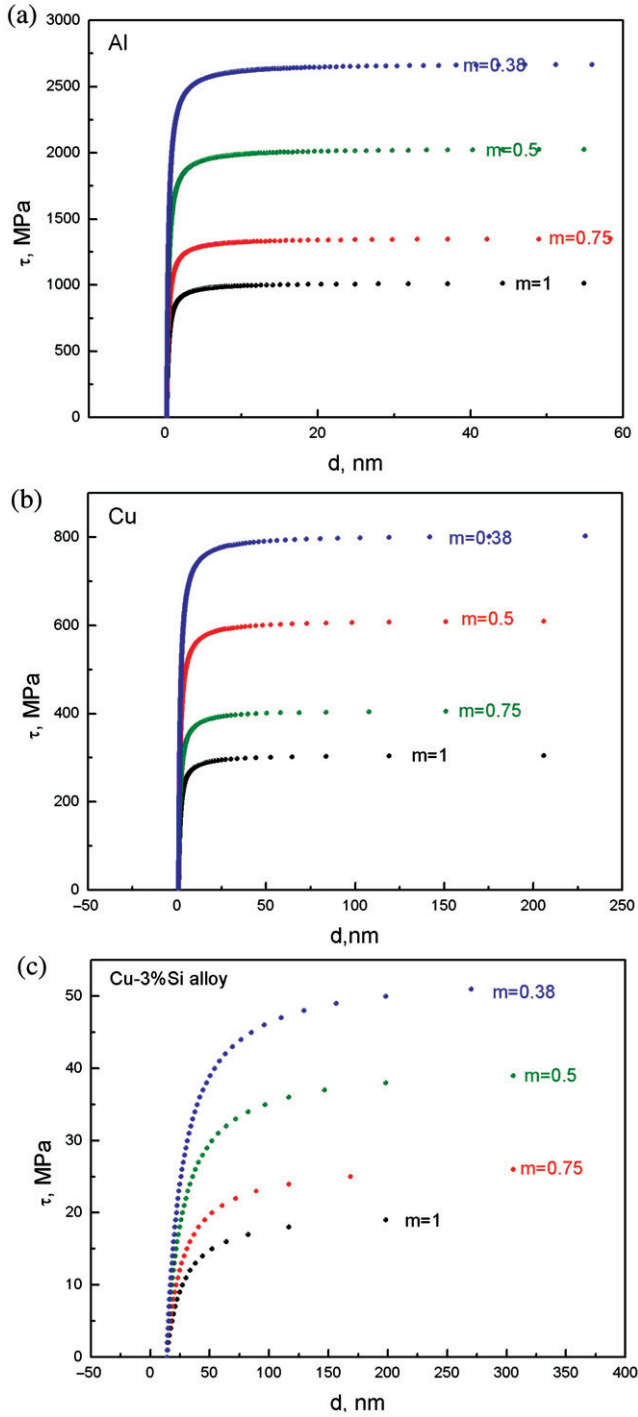


Figure 13. Plot for the variation in critical shear stress for propagating Shockley partials with the shear factor value for (a) Al, (b) Cu and (c) Cu-3% Si alloy.

to nucleate a perfect dislocation with that required to initiate a Shockley partial [23–27]. As pointed out in the previous section, this assumption is not enough to explain why deformation twins only nucleate in some grains in NC or even in single crystals or coarse-grained metals. Therefore, the effect of grain size on the behavior of deformation twinning requires further investigation.

The influence of grain size is evident mainly within the constraints of the dislocation nucleation and slip process [44,47–49]. The total applied shear stress required to activate the dislocation source is given by [44,47–49]

$$\tau_{DS} = \frac{Gb}{2R}, \quad (10)$$

where R is the radius of the dislocation source. The shear stress required to activate the dislocation source is inversely proportional to the size of the source. In ultrafine-grained or nano-grained material, the dislocation nucleates at the grain boundary and the size of dislocation source is approximately equal to the grain size. Hence, the stress required to activate a twinning dislocation in ultrafine-grained or nano-grained material can be written as

$$\tau_{DS} = \frac{Gb_p}{Dm}, \quad (11)$$

where b_p is the magnitude of Burgers vector for partial dislocation, G is the shear modulus, D is the grain size and m is the shear factor. Combining the influence of grain size with crystallographic orientation plus SFE, the twinning stress can be expressed as

$$\tau_T \geq \tau_{DS} + \tau_{SF} = \frac{Gb_p}{Dm} + \frac{\gamma}{mb_p} = \frac{1}{m} \left(\frac{Gb_p}{D} + \frac{\gamma}{b_p} \right). \quad (12)$$

Clearly, twinning stress is controlled by the combined effect of the three factors; i.e. grain size (D), SFE (γ) and shear factor (m). However, the size effect and the SFE play different roles depending on length-scale. When the grain size is larger than a certain value, say D_{C1} , the size effect only contributes a little and can be neglected in calculation. Therefore, in this case, the twinning stress in Equation (12) can be simplified as

$$\tau_T \geq \frac{\gamma}{mb_p}. \quad (13)$$

This shows that the twinning stress is mainly determined by both SFE and crystallographic orientation in coarse-grained material. Deformation twins occur in some grains with preferential orientations, and the corresponding deformation conditions can provide the required internal stress simultaneously. On the other hand, for materials with a grain size smaller than the critical size, say D_{C2} , the effect of SFE is relatively small compared to the size effect and can be neglected in calculation. In this case, the twinning stress in Equation (12) can be written as

$$\tau_T \geq \frac{Gb_p}{Dm}. \quad (14)$$

This indicates that the twinning stress is mainly determined by both size effect and crystallographic orientation when the grain size is smaller than the critical value D_{C2} .

In other words, the SFE difference can be neglected at this scale. For materials with a grain size smaller than D_{C1} and larger than D_{C2} , the twinning stresses are expressed by Equation (12). The combination of the three factors controls the twinning stresses at intermediate scales.

Distinguishing the three regions based on the factors controlling twinning stress, let us take Cu as an example. Figure 14a illustrates the variations in twinning stress and slip stress with the length-scale for those grains with the maximum shear factor. Twinning stress was calculated using Equation (12) and the slip stress was estimated by using $\tau_{\text{slip}} = Gb/Dm$, where b is the magnitude of Burgers vector for full dislocation. It is interesting to notice that the twinning stress would be equal to slip stress at a grain size of ~ 350 nm for Cu. Figure 14b shows the contribution of size effect (Equation (14)) and SFE (Equation (13)) to twinning stress. In coarse-grained material, the size effect can be neglected, as shown in Figure 14b. The value of critical grain size, D_{C1} , roughly calculated as the contribution of size effect to twinning stress, is only 1% of SFE, which leads to a D_{C1} value of $\sim 10 \mu\text{m}$ for Cu. On the other hand, the contribution of size effect increases significantly with decreasing the grain size. The value of critical grain size, D_{C2} , roughly

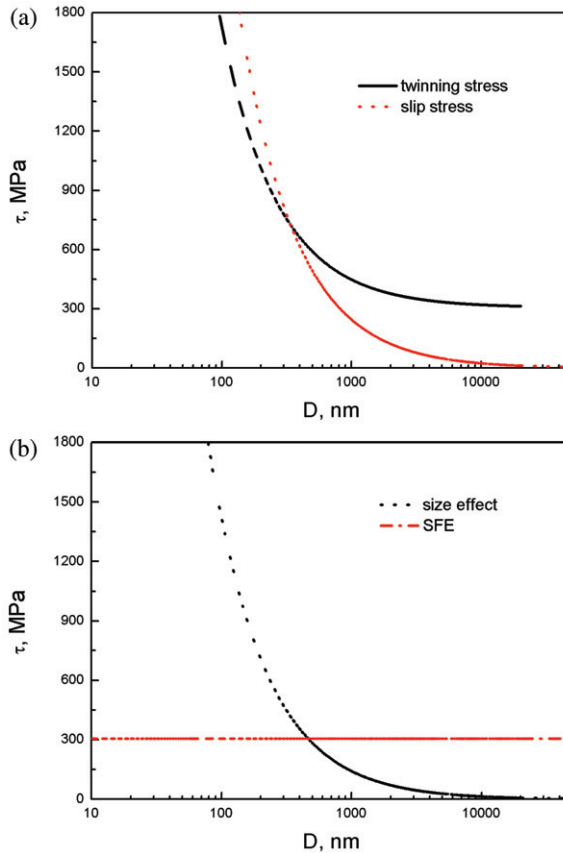


Figure 14. Plot of (a) variation in twinning stress and slip stress with grain size, (b) contribution of SFE (Equation (13)) and size effect (Equation (14)) to twinning stress with varying length-scale.

calculated as the contribution of size effect to twinning stress is 100 times SFE, resulting in a D_{C2} value of ~ 10 nm. Based on the above analysis, the three regions relative to the size effect in Cu are schematically illustrated in Figure 15. In region I, for those materials with a grain size smaller than 10 nm, both size effect and crystallographic orientation determine the twinning stress. However, twinning is not the dominant deformation mechanism because the twinning stress value is still very high. In this case, other mechanisms may be more competitive, such as a grain boundary-mediated process [22,52]. In region II, twinning stress is determined by SFE, size effect and orientation; thus, both dislocation slip and deformation twinning are the dominant deformation mechanisms. In region III, twinning stress is obviously higher than slip stress and it is determined by the SFE and crystallographic orientation. Therefore, dislocation slip becomes the dominant deformation mechanism and twinning is only regarded as a secondary deformation mode. Even if twinning stress is lower than slip stress for a grain size smaller than 350 nm in Cu, deformation twinning may not definitely occur at this scale because the grains might not have a preferential orientation.

The above analysis demonstrates that, with decreasing grain size, twinning stress increases continuously and the influence of SFE gradually decreases, whereas crystallographic orientation always plays a significant role. To judge whether twinning can nucleate in a given fcc crystal, two aspects need to be considered. One is twinning stress, whose value can be evaluated according to intrinsic factors, such as SFE, orientation and grain size. Another is applied deformation conditions. Once the external loading mode matches the required twinning stresses, twins will naturally nucleate. Thus, it is easy to understand the contradictory experimental results on the size effect. For grain sizes between 1 and $10\ \mu\text{m}$, the required twinning stress increases with decreasing grain size, while, during plastic deformation, internal stresses hardly accumulate to the required twinning stress level [11,13]. However, for materials with ultrafine- or nano-grained sizes, the required twinning stress further increases with decreasing grain size but the accumulated internal stress increases rapidly due to size effect (slip stress becomes larger than twinning stress at this scale); therefore, deformation twinning becomes a relatively easier deformation mode [19–27].

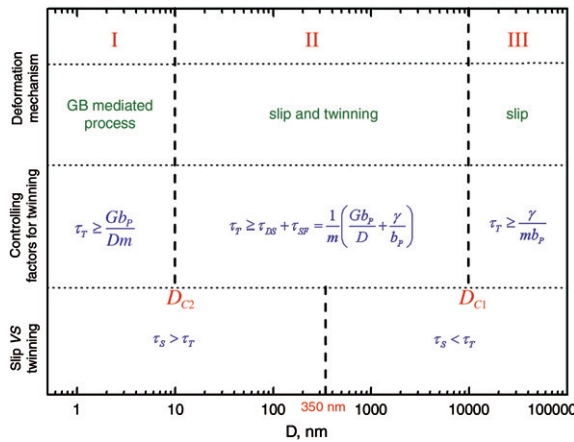


Figure 15. Three regions classified according to the influence of size effect.

5. Conclusions

Three types of fcc crystal with different SFEs and crystallographic orientations were subjected to single-pass ECAP and literature references on the grain-size effect, and reviewed to investigate the combined effects of SFE, crystallographic orientation and grain size on deformation twinning behavior. Based on the experimental observations and analyses, the following conclusions are drawn:

- (1) Crystallographic orientation and SFE significantly influence the process of deformation twinning in fcc crystals. For Al single crystals, no deformation twins were found to nucleate, although a preferential crystallographic orientation was selected, indicating that SFE plays a critical role in deformation twinning. For Cu single crystals, numerous deformation twins were observed, although it was extruded for a single-pass only at RT and low strain rate, demonstrating that crystallographic orientation is one of the main controlling factors. For the Cu-3% Si alloy, deformation twins were only found in some grains and others were full of planar dislocations, although it has the lowest SFE value, showing again that deformation twinning is controlled by the combined effects of SFE and crystallographic orientation.
- (2) Further analysis based on fundamental dislocation mechanisms indicates that twinning stress is mainly controlled by three intrinsic factors: SFE, crystallographic orientation and grain size. With decreasing grain size, twinning stress increases continuously and the influence of SFE gradually decreases, whereas crystallographic orientation always plays an important role in deformation twinning.

Acknowledgements

The authors thank Professor Li GY for his valuable discussions. This work was supported by the National Natural Science Foundation of China (NSFC) under grant Nos. 50471082, 50371090 and 50571102. ZFZ would like to acknowledge the financial support of 'Hundred of Talents Project' by the Chinese Academy of Sciences and the National Outstanding Young Scientist Foundation under grant No. 50625103.

References

- [1] R.W.K. Honeycomb, E. (ed.), *Plastic Deformation of Metals*, Cambridge University Press, Cambridge, 1969.
- [2] R.Z. Valiev, R.K. Islamgaliev and I.V. Alexandrov, *Prog. Mater. Sci.* 45 (2000) p.103.
- [3] K. Lu and J. Lu, *Mater. Sci. Eng. A* 375 (2004) p.38.
- [4] R.E. Reed-Hill, J.P. Hirth, H.C. Rogers (eds.), *Deformation Twinning*, Gordon and Breach, New York, 1964.
- [5] J.W. Christian and S. Mahajan, *Prog. Mater. Sci.* 39 (1995) p.1.
- [6] T.H. Blewitt, R.R. Coltman and J.K. Redman, *J. Appl. Phys.* 28 (1957) p.651.
- [7] S.K. Varma, V. Caballero, J. Ponce et al., *J. Mater. Sci.* 34 (1996) p.5623.
- [8] V. Caballero and S.K. Varma, *J. Mater. Sci.* 34 (1999) p.461.
- [9] M.A. Meyers, O. Vohringer and V.A. Lubarda, *Acta Mater.* 49 (2001) p.4025.
- [10] A. Rohatgi, S.K. Vecchio and G.T. Gray III, *Metall. Mater. Trans. A* 32 (2001) p.135.
- [11] E. El-Danaf, S.R. Kalidindi and R.D. Doherty, *Metall. Mater. Trans. A* 30 (1999) p.1223.
- [12] Y.M. Wang, T. Jiao and E. Ma, *Mater. Trans.* 44 (2003) p.1926.

- [13] M.A. Meyers, R.U. Andrade and H.A. Chokshi, *Metall. Mater. Trans. A* 26 (1995) p.2881.
- [14] J.C. Sanchez, L.E. Murr and K.P. Staudhammer, *Acta Mater.* 45 (1997) p.3223.
- [15] O. Johari and G. Thomas, *Acta Metall.* 12 (1964) p.1153.
- [16] M.A. Crimp, B.C. Smith and D.E. Mikkola, *Mater. Sci. Eng.* 96 (1987) p.27.
- [17] G.T. Gray III, P.S. Follansbee and C.E. Frantz, *Mater. Sci. Eng. A* 111 (1989) p.9.
- [18] L.E. Murr and E.V. Esquivel, *J. Mater. Sci.* 39 (2004) p.1153.
- [19] V. Yamakov, D. Wolf, S.R. Phillpot et al., *Nat. Mater.* 1 (2002) p.45.
- [20] V. Yamakov, D. Wolf, S.R. Phillpot et al., *Acta Mater.* 50 (2002) p.5005.
- [21] J. Schiøtz and K.W. Jacobsen, *Science* 301 (2003) p.1357.
- [22] H. Van Swygenhoven, *Science* 296 (2002) p.66.
- [23] M.W. Chen, E. Ma, K.J. Hemker et al., *Science* 300 (2003) p.1257.
- [24] C.X. Huang, K. Wang, S.D. Wu et al., *Acta Mater.* 54 (2006) p.655.
- [25] X.Z. Liao, Y.H. Zhao, S.G. Srinivasan et al., *Appl. Phys. Lett.* 84 (2004) p.592.
- [26] X.Z. Liao, F. Zhou, E.J. Lavernia et al., *Appl. Phys. Lett.* 83 (2003) p.632.
- [27] X.Z. Liao, F. Zhou, E.J. Lavernia et al., *Appl. Phys. Lett.* 83 (2003) p.5026.
- [28] N. Hansen, *Metall. Mater. Trans. A* 32 (2001) p.2917.
- [29] Q. Liu and N. Hansen, *Phys. Status Solidi A* 149 (1995) p.187.
- [30] Q. Liu, D.J. Jensen and N. Hansen, *Acta Mater.* 46 (1998) p.5819.
- [31] F.J. Humphreys and M. Hatherly, *Recrystallization and Related Annealing Phenomena*, Great Yarmouth, Galliard, 1995.
- [32] V.M. Segal, *Mater. Sci. Eng. A* 197 (1995) p.157.
- [33] V.M. Segal, *Mater. Sci. Eng. A* 345 (2003) p.36.
- [34] W.Z. Han, Z.F. Zhang, S.D. Wu et al., *Acta Mater.* 55 (2007) p.5889.
- [35] W.Z. Han, Z.F. Zhang, S.D. Wu et al., *Mater. Sci. Eng. A* 476 (2008) p.224.
- [36] G.J. Fan, H. Choo, P.K. Liaw et al., *Acta Mater.* 54 (2006) p.1759.
- [37] D.R. Fang, Z.F. Zhang, S.D. Wu et al., *Mater. Sci. Eng. A* 426 (2006) p.305.
- [38] W.Z. Han, Z.F. Zhang, S.D. Wu, et al., *Adv. Eng. Mater.* (2008), in press.
- [39] H. Miyamoto, U. Erb, T. Koyama et al., *Phil. Mag. Lett.* 84 (2004) p.235.
- [40] M. Wróbel, S. Dymek and M. Blicharski, *Scripta Mater.* 35 (1996) p.417.
- [41] S. Dymek and M. Wróbel, *Mater. Chem. Phys.* 81 (2003) p.552.
- [42] A.S. Malin, M. Hatherly, P. Welch et al., *Z. Metall.* 73 (1982) p.489.
- [43] Z. Gronostajski and K. Jaskiewicz, *Arch. Metall.* 48 (2003) p.435.
- [44] J.P. Hirth and J. Lothe, *Theory of Dislocations*, Wiley, New York, 1991.
- [45] V. Yamakov, D. Wolf, M. Salazar et al., *Acta Mater.* 49 (2001) p.2713.
- [46] T.S. Byun, *Acta Mater.* 51 (2003) p.3063.
- [47] A.H. Cottrell and B.A. Bilby, *Phil. Mag.* 42 (1951) p.573.
- [48] J.A. Venables, *Phil. Mag.* 63 (1961) p.379.
- [49] K.P.D. Lagerlof, J. Castaing, P. Pirouz et al., *Phil. Mag. A* 82 (2002) p.2841.
- [50] M.S. Szczerba, T. Bajor and T. Tokarski, *Phil. Mag.* 84 (2004) p.481.
- [51] Y. Fukuda, K. Oh-ishi, M. Furukawa et al., *Acta Mater.* 52 (2004) p.1387.
- [52] Z.W. Shan, Z.W. Stach, J.M.K. Wiezorek et al., *Science* 305 (2004) p.654.